RAMReS Sciences des Structures et de la Matière Vol. 6, N°1 (2022) 47- 62
http://publication.lecames.org/index.php/mat ISSN: 2630-1180

Voltammetric and chronoamperometric study of omnipaque electrooxidation at Ti/RuO_2 electrode

Kouakou Jocelin Kimou[1], Ollo Kambiré[2], Sylvestre Konan Koffi[1], Souleymane Koné[1], Lassiné Ouattara[1,*]

[1]Laboratoire de constitution et réaction de la matière, UFR SSMT, Université Félix Houphouët-Boigny, Abidjan, 22 BP 582 Abidjan 22, Côte d'Ivoire
[2]UFR Sciences et Technologies, Université de Man, BP 20 Man, Côte d'Ivoire

Received: 20 January 2022 / Received in revised form: 22 March 2022 / Accepted: 15 April 2022

***Abstract*:**

Electrochemical methods have shown their effectiveness in the prevention and resolution of wastewater contamination problems. However, before the electrolysis of an organic pollutant (Omnipaque: OMP) by this method, it is necessary to know the electrochemical behavior of this pollutant. Thus, the objective of this work is to contribute to the understanding of the electrochemical phenomena occurring at the electrode/electrolyte interface during the electrooxidation of omnipaque. The study was carried out using voltammetry and chronoamperometry. In this study, Ti/RuO_2 electrode was prepared on titanium (Ti) substrate by thermal decomposition techniques at 400 °C. The prepared electrode was characterized by scanning electron microscopy (SEM) and electrochemistry. These characterizations showed the presence of RuO_2 on the electrode surface. The electrochemical study has shown that the oxidation of omnipaque is done following a direct electronic transfer on the surface of the electrode by an adsorption-diffusion coupling of the electroactive species on the surface of the electrode. OMP electrooxidation includes the exchange of three protons and five electrons in acidic media and two protons and one electron exchanged in basic media. We note the activation of several active sites on RuO_2 surface as well as the intervention of hydroxyl radicals in the catalytic electrooxidation process of OMP with increasing temperature. The values of activation energy and catalytic rate constant were estimated as 7.895 kJ/mol and 82.2 M^{-1} s^{-1}, respectively.

***Keywords*:** Cyclic voltammetry; Chronoamperometry; Omnipaque; Ruthenium dioxide; Electrooxidation.

*Corresponding author:
Email address: ouatlassine@yahoo.fr *(L. Ouattara)*

1. Introduction

Recently, the scientific community has focused on the fate of organic products, more specifically pharmaceuticals, after use [1-5]. Indeed, several studies have shown the presence of pharmaceuticals in surface waters and the potential hazards to which humans and aquatic beings are exposed [6, 7]. Among the pharmaceuticals, iodinated contrast (IC) are a class of products that are increasingly studied [8-12]. ICs are widely used in health centers for visualization of organs and blood vessels. ICs are excreted virtually unchanged from the body after injection [6]. One of the most commonly used of ICs in medical imaging centers is iohexol known in the pharmaceutical industry under the chemical formulation of omnipaque. According to the literature several studies have shown the presence of omnipaque in hospital wastewater and surface water [13, 14].

A general awareness is therefore necessary in order to propose efficient treatment methods for hospital wastewater and surface water containing pharmaceutical pollutants.

According to the literature [13, 15-18], several techniques such as physical, biological and chemical methods used in wastewater treatment are ineffective against toxic and difficult to biodegradable compounds.

In this context, electrochemical methods are indicated because they are known to be effective in preventing and solving wastewater contamination problems [3, 19].

According to the literature, it should be noted that the use of these techniques imply the choice of the electrode to be used as anode. The boron-doped diamond electrode has shown its efficiency in the oxidation of pharmaceutical pollutants [3]. However, the very high cost of this electrode limits its use in electrochemistry despite its very good electrochemical properties [20]. Thus, in recent years, research has turned to new electrodes called dimensionally stable anodes (DSA) with high electrocatalytic activities, high stability against anodic corrosion and also very high mechanical stability [21, 22]. Among the DSAs, ruthenium dioxide electrode (RuO_2) with relatively affordable cost [2] and interesting chemical and electrochemical properties such as high lifetime, resistance against acid corrosion and high electrocatalytic activity for the organic compounds oxidation [21] has been widely used for the oxidation and degradation of pharmaceuticals such as paracetamol and amoxicillin [2, 21, 23].

In this work, the study of the electrochemical behavior of OMP by cyclic voltammetry and chronoamperometry on Ti/RuO_2 electrode was performed. The effect of scan rate, OMP concentration, temperature and pH on OMP electrooxidation on Ti/RuO_2 electrode were investigated.

2. Experimental

2.1. Preparation of Ti/RuO_2 electrode

Ti/RuO_2 electrode was prepared by dissolving the precursor solution ($RuCl_3.3H_2O$) in 10 mL of isopropanol. The dimensions of the titanium substrate used are 1.6 cm x 1.6 cm x 0.5 cm. Titanium surface was sandblasted to facilitate the adhesion of the precursor solution. After this step, the titanium substrate was washed with water and isopropanol to remove the sand grains on the titanium surface. The titanium substrates are oven dried at 80 °C for 10 min. Then, the precursor solution is applied on the surface of the treated substrate with a brush. In detail, the preparation of the electrodes is as follows: (i) Application of the solution with a brush, on the treated surface; (ii) Baking at 80 °C for 10 min to evaporate the solvent; (iii) Thermolysis in an oven at 400 °C for 15 min; (iv) Removal from the oven and cooling. The operations succession from (i) to (iv) constitutes the deposition protocol for one layer. More than three sequential layers are deposited to ensure a good coverage of the substrate. The final step consists in a calcination at 400 °C during one hour under the ambient atmosphere of the oven.

2.2. Measurement methods

The electrochemical study is carried out using an experimental device composed of an Autolab Potentiostat of ECHOCHEMIE (PGSTAT 20), interfaced with a computer. The electrochemical measurements were performed in a three-electrode cell. The working electrode was Ti/RuO_2 electrode, the counter electrode was a platinum wire, and the reference electrode was a saturated calomel electrode (SCE). To overcome the potential ohmic drop, the reference electrode was mounted in a luggin capillary and placed close to the working electrode by a distance of 1 mm. The apparent exposed area of the working electrode was 1 cm^2. An MGW LAUDA thermoregulator connected to the electrochemical cell was used for temperature variation. The pH of the electrolytes was measured using a HI2211 pH meter equipped with a glass electrode probe.

2.3. Chemicals

Omnipaque (iohexol) 300 mg I/ml manufactured by GE Healthcare Ireland with the empirical formula $C_{19}H_{29}0_9N_3I_3$ was purchased from a drugstore in Abidjan (Côte d'Ivoire). Sodium hydroxide (NaOH) was manufactured by the company Merck. Sulfuric acid (H_2SO_4) was supplied by the company Fluka. All solutions were prepared with distilled water.

3. Results and discussion

3.1. Physical characterization

The surfaces of bare titanium plates, bare sandblasted titanium, and precursor solution ($RuCl_3.3H_2O$) modified titanium plates were

analyzed by scanning electron microscopy (SEM). The obtained images are shown in Figure 1. The bare titanium plate (Figure 1A) has a smooth structure that prevents the deposition of the precursor solution on its surface. Therefore, this structure of the titanium should be modified by sandblasting. The sandblasted titanium plate Figure 1B has a rough structure with the presence of asperities that could facilitate the adhesion of the ruthenium precursor solution. For the Ti/RuO_2 electrode (Figure 1C), a change in appearance is observed characterized by pores, a rough and cracked surface. The cracking observed on the Ti/RuO_2 surface is believed to be due to thermal shock during removal of the plates from the furnace [2, 21]. It is also noted that the titanium surface is not visible in Figure 1C. This shows that the surface of the support is completely covered by RuO_2.

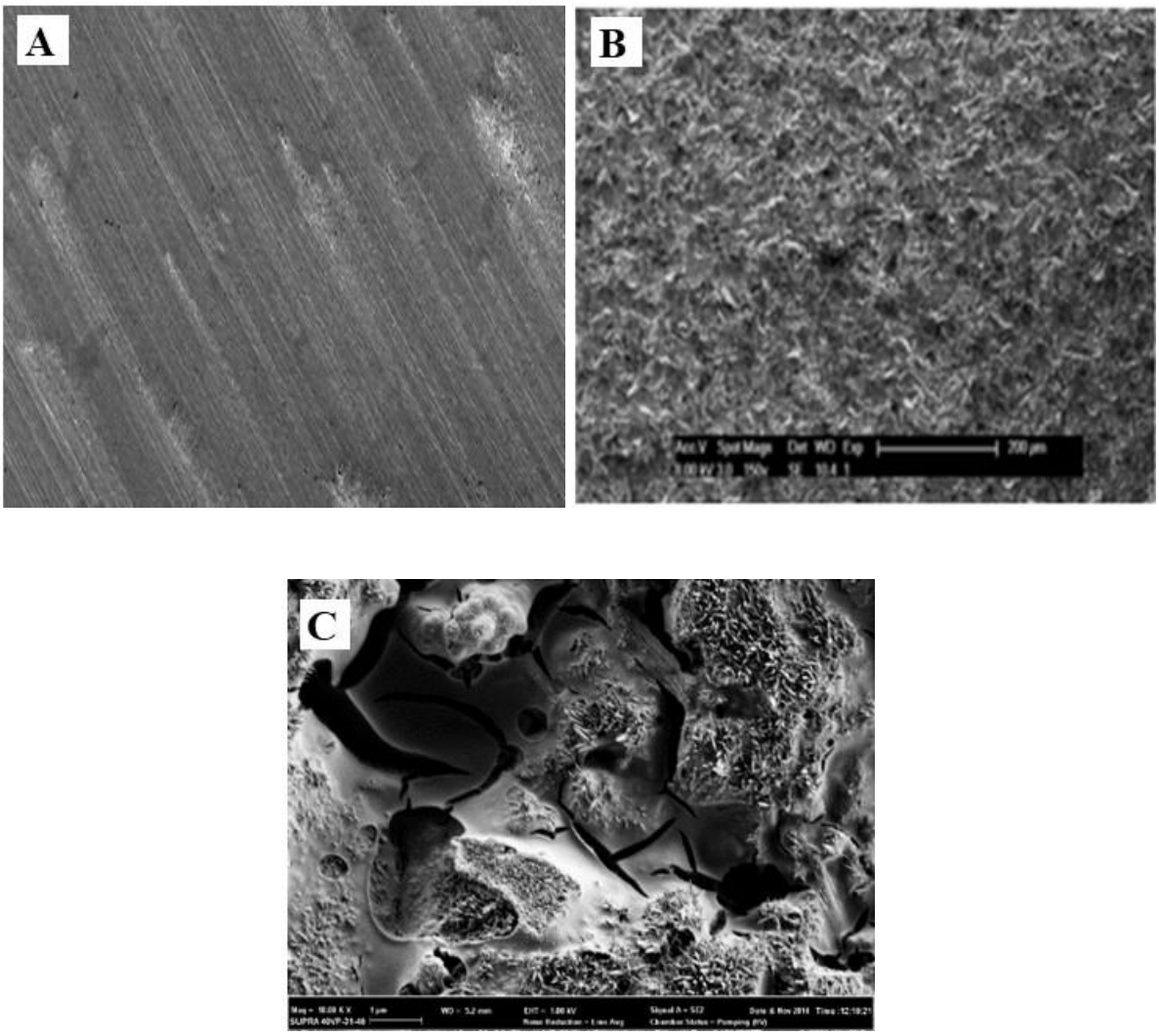

Fig. 1. (A) SEM of unsandblasted titanium, (B) Sandblasted titanium and (C) Ti/RuO_2 electrode.

3.2. Voltammetric study

3.2.1. Voltammetric behaviour of OMP at Ti/RuO₂

Figure 2 represents the cyclic voltammogram of Ti/RuO_2 in sulfuric acid (0.1 M) in the presence and absence of OMP.

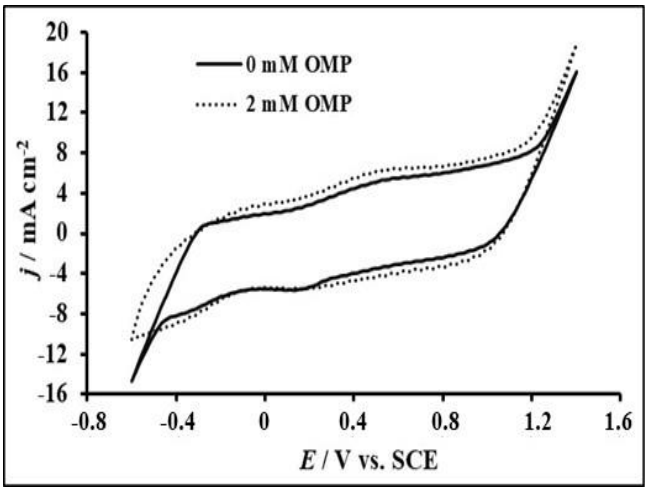

Fig. 2. Cyclic voltammograms of Ti/RuO_2 in 0.1 M H_2SO_4 in presence and absence of OMP at 50 mV/s, CE: platinum wire, RE: SCE, T = 25 °C.

In the absence of OMP, the voltammogram shows a low intensity oxidation wave around 0.6 V vs. SCE in the forward potential scan and a low intensity reduction wave around 0.16 V vs. SCE. The presence of these waves could be due respectively to the redox transitions of Ru (III) / Ru (IV) and (Ru (IV) / Ru (III) on RuO_2 electrode surface [2, 21, 24]. This voltammogram is identical to that obtained in our previous work with the RuO_2 electrode [2, 24]. This result confirms the presence of RuO_2 on our electrode. In the absence of OMP, oxygen evolution reaction begins at 1.23 V vs. SCE characterized by a rapid increase in current density. In the presence of 2 mM OMP, there is an increase in voltammetric charge and a decrease in the onset of oxygen evolution reaction potential.

3.2.2. Influence of potential scan rate

Figure 3 shows the results obtained for different scan rates in H_2SO_4 (0.1 M) containing 3.2 mM OMP. This figure shows that the current density increases and the voltammetric charge increase with the scan rate. At a given potential of 0.6 V vs. SCE, figure 4A shows the current density (j) as a function of the square root of the potential scan rate ($v^{1/2}$). Figure 4B shows the logarithm of the current density (ln j) as a function of the logarithm of the potential scan rate (ln v) to study the kinetic regime [23, 25].

The curve j *vs.* $v^{1/2}$ obtained is a straight line with determination coefficient $R^2 = 0.9867$. The value of the determination coefficient shows the good linearity between the current density and the square root of the potential scan rate. However, the obtained straight line does not intercept the origin of the axes, indicating that the electrooxidation process of OMP could be controlled by adsorption [26, 27].

To confirm the kinetic regime, the curve of ln j vs. ln v was plotted and shown in Figure 4B. The obtained curve is a straight line with equation:

$$\ln j = 0.553 \ln v + 2.872 \quad (R^2 = 0.988) \qquad (1)$$

The value of the slope 0.553 close to 0.5 indicates that the process at the electrode is controlled by diffusion [27-29]. Therefore, it can be concluded that the OMP electrooxidation is a process controlled by an adsorption-diffusion coupling on the Ti/RuO_2 surface.

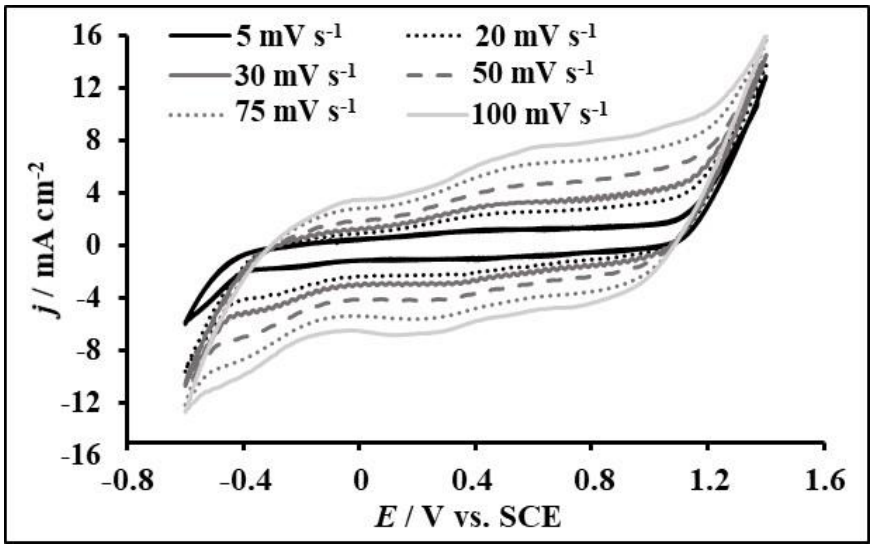

Fig. 3. Cyclic voltammograms of Ti/RuO_2 in 0.1 M H_2SO_4 containing 3.2 mM OMP at different scan rate, CE: platinum wire, RE: SCE, T = 25°C.

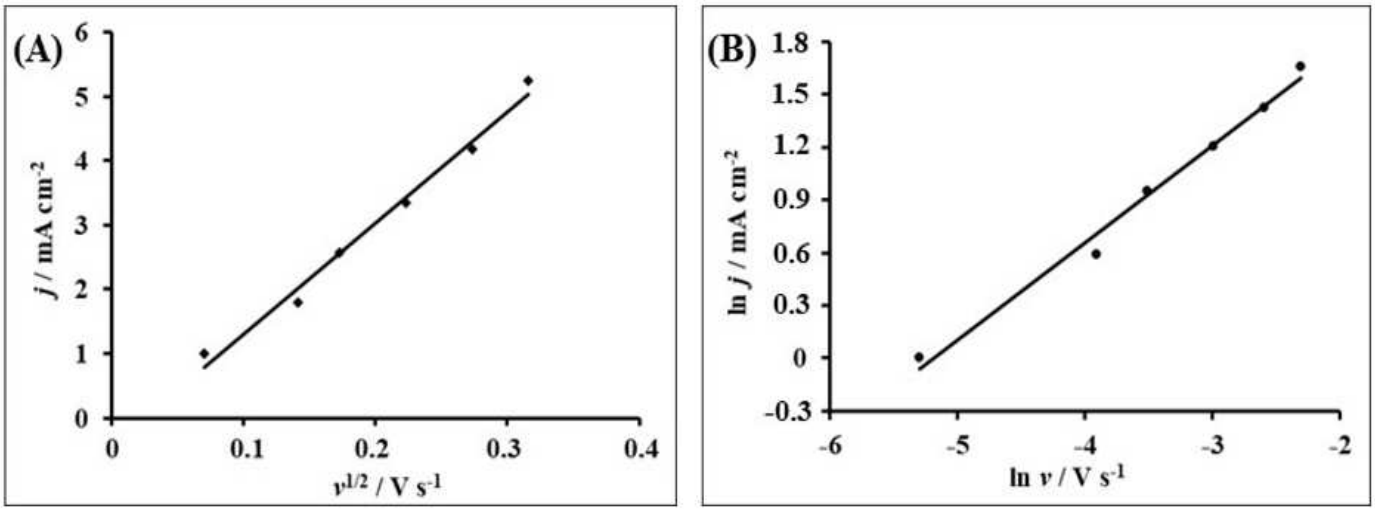

Fig. 4. (A) Current density as a function of the square root of the potential scan rate; (B) ln *j* vs. ln *v* plot.

3.2.3. Influence of OMP concentration

In Figure 5A, voltammograms are made in H_2SO_4 media in the presence of several concentrations of OMP at 50 mV/s. At a potential of 0.6 V vs. SCE, we note a rapid increase of the current density going from 3.97 mA cm^{-2} for 1.2 mM OMP to 7.8 mA cm^{-2} for 3.2 mM OMP. Moreover, we note the presence of an oxidation wave around 0.6 V vs. SCE which could indicate the oxidation of the electrode and the adsorption-oxidation of the OMP.

The difference between the oxygen evolution potential in the presence (E) and absence (E_0) of OMP ($E-E_0$) for a current density of 10 mA cm^{-2} was determined for OMP several concentrations. The results obtained are presented in Table 1. According to this table, the $E-E_0$ difference decreases with the OMP concentration. This shows that increasing the OMP concentration shifts the oxygen evolution reaction to the negative values of the potential. This also reflects the intervention of oxidative species such as hydroxyl radicals resulting from the electrochemical decomposition of water in the oxidation of OMP [23].

On the other hand, the current density was plotted as a function of OMP concentration at a potential of 0.6 V vs. SCE (Figure 5B). The curve obtained is a straight line described by the following equation:

$$j = 1.811\ C + 2.0081 \quad (R^2 = 0.9584) \qquad (2)$$

The determination coefficient ($R^2 = 0.958$) close to 1 shows that the current density is proportional to OMP concentration. This indicates that the increase in current density reflects the OMP oxidation. The increase in current density in the electroactivity range of the anode shows that OMP is oxidized directly by electronic transfer on the surface of Ti/RuO_2 in the water stability range. Therefore, OMP can be degraded by a catalytic oxidation mechanism involving direct oxidation of this pollutant on the Ti/RuO_2 surface.

Table 1
Value of $E - E_0$ as a function of OMP concentration (j = 10 mA cm^{-2})

OMP Concentration (mM)	$\lvert E - E_0 \rvert$ (V vs. SCE)
1.2	0.044
1.6	0.097
2	0.156
2.8	0.214
3.2	0.282

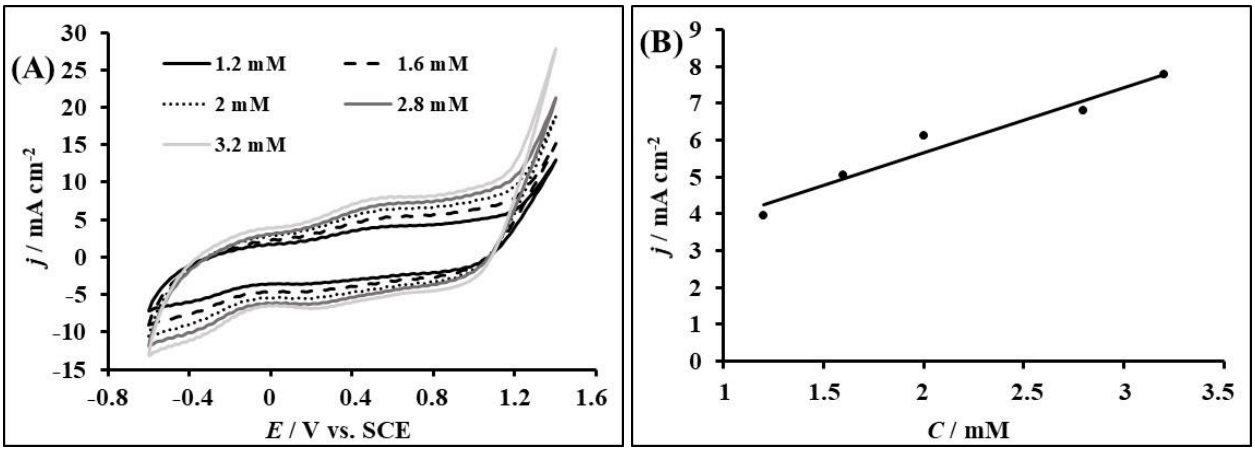

Fig. 5. (A) Cyclic voltammetry curves recorded on Ti/RuO_2 in H_2SO_4 (0.1 M) in the presence of different OMP concentrations at 50 mV / s; (B) Plot of *j* vs. *C*.

3.2.4. Effect of temperature

The effect of temperature on the OMP electrooxidation was studied in H_2SO_4 (0.1 M) in the presence of 3.2 mM OMP at 50 mV/s. The obtained voltamograms are presented by Figure 6A. Between 0 and 0.8 V vs. SCE, an increase in current density with temperature is observed. This increase in current density marked by the appearance of anodic wave could be attributed to the OMP oxidation. The current of the OMP oxidation peak increases with temperature. On the other hand, the oxygen evolution reaction potential decreases with increasing temperature reflecting an improvement of oxygen evolution reaction with temperature. These results can be explained by the *in-situ* production of hydroxyl radicals by electrochemical decomposition of water and/or by the activation of several active sites on the Ti/RuO_2 surface. Indeed, with the rise in temperature, there is an interpenetration of the electrolytic solution in the internal layers of RuO_2 deposit. The plot of the logarithm of the peak current density as a function of the inverse of temperature ($\ln j = f(1/T)$) is shown in Figure 6B.

The curve $\ln j = f(1/T)$) obtained is a straight line showing a linear relationship between $\ln j$ and the inverse of the temperature:

$$\ln j = -949.631\ 1/T + 4.644\ (R^2 = 0.9517) \qquad (3)$$

The value of the activation energy (Ea) was calculated using the slope of equation (3) and the following relationship [30]:

$$E_a = -R\left(\frac{\partial \ln j}{\partial (1/T)}\right) \qquad (4)$$

Where, R is the universal gas constant (8.314 J K^{-1} mol^{-1}).

We obtain a value of 7.895 kJ/mol. The value of Ea lower than 40 kJ/mol gives information about the kinetic regime which would be controlled by diffusion [31, 32].

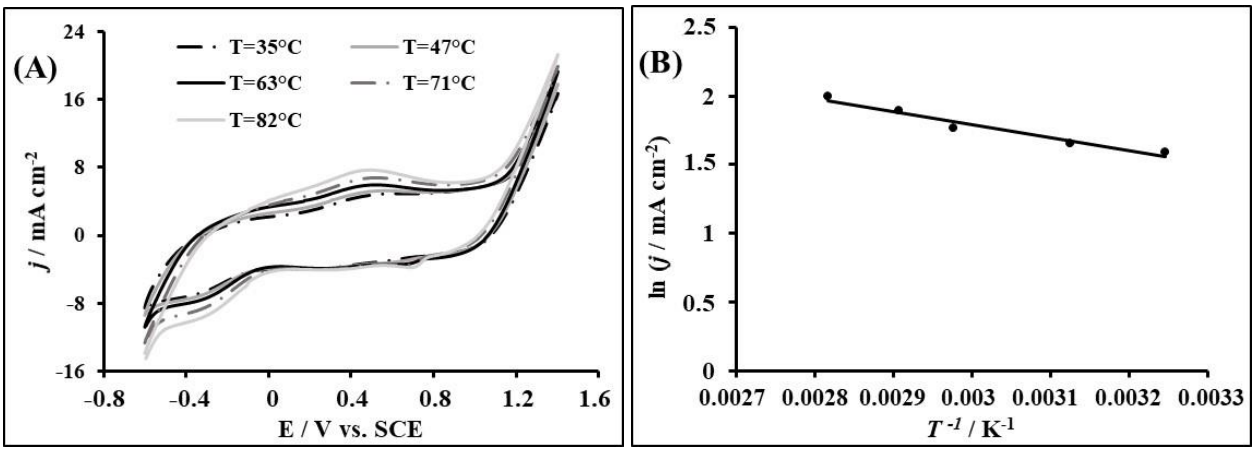

Fig. 6. (A) Cyclic voltammograms of Ti/RuO_2 in 0.1 M H_2SO_4 containing 3.2 mM OMP at several temperatures at 50 mV/s. CE: platinum wire, RE: SCE; (B) plot of ln *j* vs. *1/T*.

3.2.5. Effect of pH

The study of the pH influence on the electrooxidation of OMP was performed. The results of pH range from 2 to 12.4 in H_2SO_4 solution (0.1 M) containing 3.2 mM OMP were shown in Figure 7A. With the increase of the pH, a decrease of the current density is observed for pH values (from 2 to 5.9), then the current density increases with the pH for basic solutions. In basic medium, a progressive modification of the voltamograms appears clearly with a disappearance of the oxidation wave of the redox transitions and an appearance of an oxidation wave at 0.6 V vs. SCE and of an oxidation peak at 0.9 V vs. SCE. The presence of this wave and the oxidation peak could indicate that the OMP oxidation would be favorable in basic environment and that a detection of OMP would be easier at basic solution on the Ti/RuO_2 electrode.

For a current density of 5 mA cm^{-2}, the potential versus pH curve was plotted (Figure 7B). The curve obtained is a juxtaposition of two half lines described by equation (5) in acidic media and equation (6) in basic media.

$E = 0.039\ pH + 1.051$ $(R^2 = 0.918)$ (5)

$E = -0.113\ pH + 1.943$ $(R^2 = 0.999)$ (6)

The presence of these two half-lines suggests different oxidation mechanisms for acid and basic pH.

The number of electrons and protons exchanged were calculated using the slopes (in absolute value) of the equations (5) and (6) for the two media and from the following expression [26]:

$$\frac{dEp}{dpH} = \frac{2.303mRT}{nF} \quad (7)$$

Where, m/n represents the ratio of the number of protons (m) and electrons (n) exchanged, T is the temperature in Kelvin (298 K) and F is Faraday's constant (96487 C mol^{-1}).

In acidic media, the obtained ratio m/n (0.65 $\approx$ 0.6) indicates an exchange of 3 protons for 5 electrons.

For basic values, the m/n ratio is equal to 1.9$\approx$2. The value of the ratio could indicate 2 protons exchanged for 1 electron.

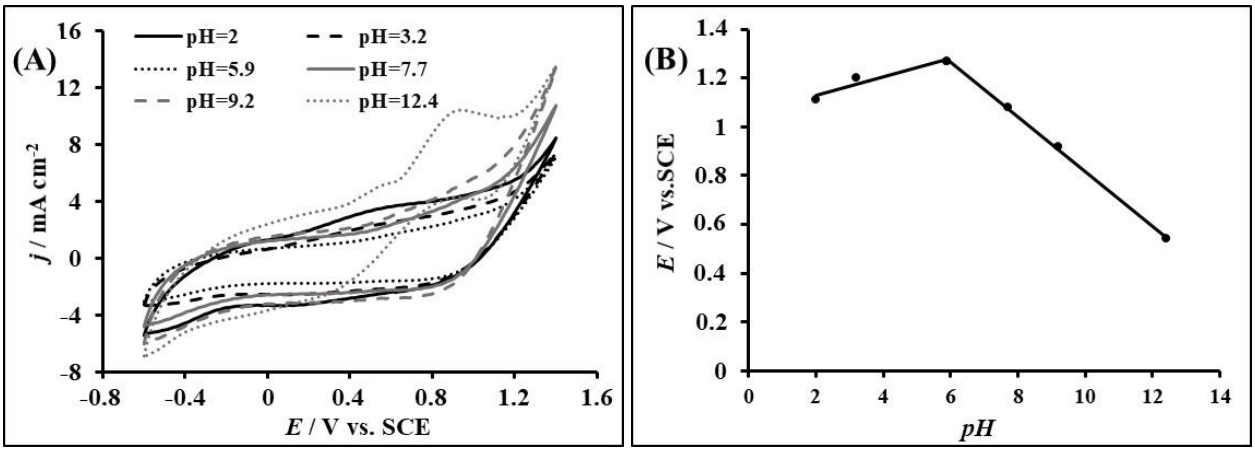

Fig. 7. (A) Cyclic voltammograms recorded on Ti/RuO_2 at different pH containing 3.2 mM OMP at 50 mV/s; (B) Peak potential as a function of pH.

3.3 Chronoamperometric study

In order to get more information about the electrocatalytic oxidation of OMP and the stability of the Ti/RuO_2 electrode, chronoamperometric measurements were performed.

The curves of current density versus time (j vs. t) obtained in H_2SO_4 media in the absence and presence of 3.2 mM OMP are presented in figure 8. The curves obtained show two parts: a rapid drop in current density (faradic current) for 10 seconds, and then a stationary current density for longer times [33]. According the literature, these observations could be respectively explained by a discharge of the electric double layer and by a diffusion of the ions present in solution [34]. Indeed, the decrease in the current density to very low values could be due to a blocking of the electrode surface by a polymeric film deposit during the oxidation of OMP [35].

In the presence of OMP, there is an increase in both faradic and stationary current densities probably due to an oxidation of the pollutant and/or more activation of active sites on Ti/RuO_2.

The values of current densities were recorded as a function of potential in a range from 0.1 to 1 V vs. SCE to determine the value of the potential corresponding to the largest value of the current density. The values obtained are recorded in Table 2. According to the values in this table, the highest current density is obtained for a potential equal to 1 V vs. SCE. Thus, all measurements will be made at a fixed potential of 1 V vs. SCE.

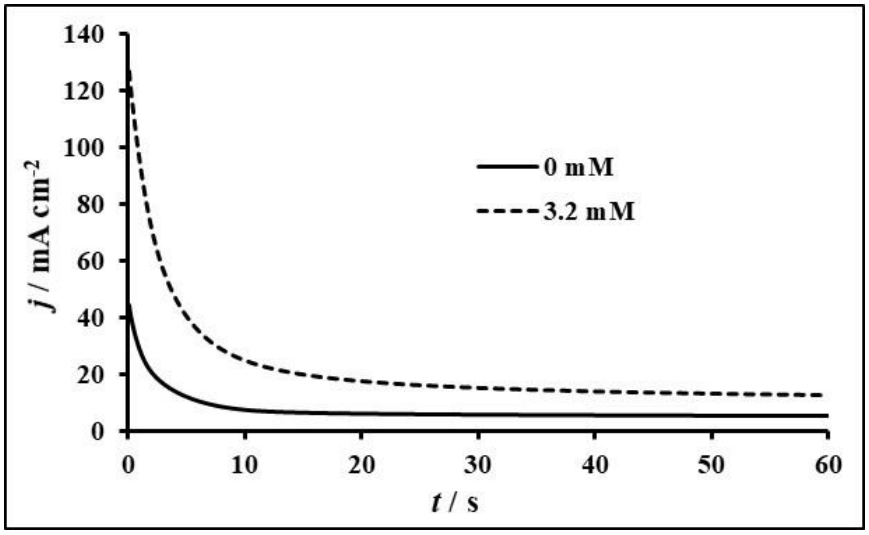

Fig. 8. Chronoamperometric curves in H_2SO_4 (0.1 M) in the absence and presence of 3.2 mM OMP at a potential of 0.3 V vs. SCE.

Table 2
Stationary current density for different potentials

E / V vs. SCE	0.1	0.2	0.3	0.4	0.5	0.6	0.7	0.8	0.9	1.0
j / mA cm^{-2}	36	16	26	32	40	55	66	80	110	116

Figure 9A shows the chronoamperometric curves obtained at a potential of 1 V vs. SCE in a H_2SO_4 solution (pH = 9) containing different concentrations of OMP. An increase in stationary current density with OMP concentration is observed suggesting that the Ti/RuO_2 electrode has a stable electrocatalytic activity for the oxidation of the pollutant [36].

The plot of stationary current density versus concentration shown in Figure 9B is a straight line described by the following equation:

$$j = 4.2878\ C - 1.2616 \quad (R^2 = 0.9813) \qquad (8)$$

Chronoamperometry was also used to determine the value of the catalytic rate constant k_{cat} , at the electrode/electrolyte interface. For an intermediate time, when the kinetic of the electrocatalytic reaction dominates the oxidation current density, the OMP electrooxidation, the catalytic current density j_{cat} can be defined by the following equation [37]:

$$\frac{j_{cat}}{j_L} = \pi^{1/2}(k_{cat} \times C_0 \times t)^{1/2} \qquad (9)$$

Where, j_{cat} and j_L represent the current densities in the presence and absence of OMP, respectively. k_{cat}, the catalytic rate constant (M^{-1} s^{-1}), C_0, the concentration of OMP (M) and t, the elapsed time (s).

The curve j_{cat} / j_L vs $t^{1/2}$ represented on Figure 10 is a straight line described by the following equation:

$j_{cat} / j_L = 0.9065\ t^{1/2} + 5.039$ ($R^2 = 0.993$) (10)

The value of the catalytic kinetic constant k_{cat} was calculated from the slopes of equations (9) and (10).

The value of k_{cat} obtained is 82.2 M^{-1} s^{-1}, which is relatively lower than those obtained on boron doped diamond electrode (BDD) during the electrochemical oxidation of OMP [34] suggesting that the Ti/RuO_2 has a less electrocatalytic activity for OMP electrooxidation [36].

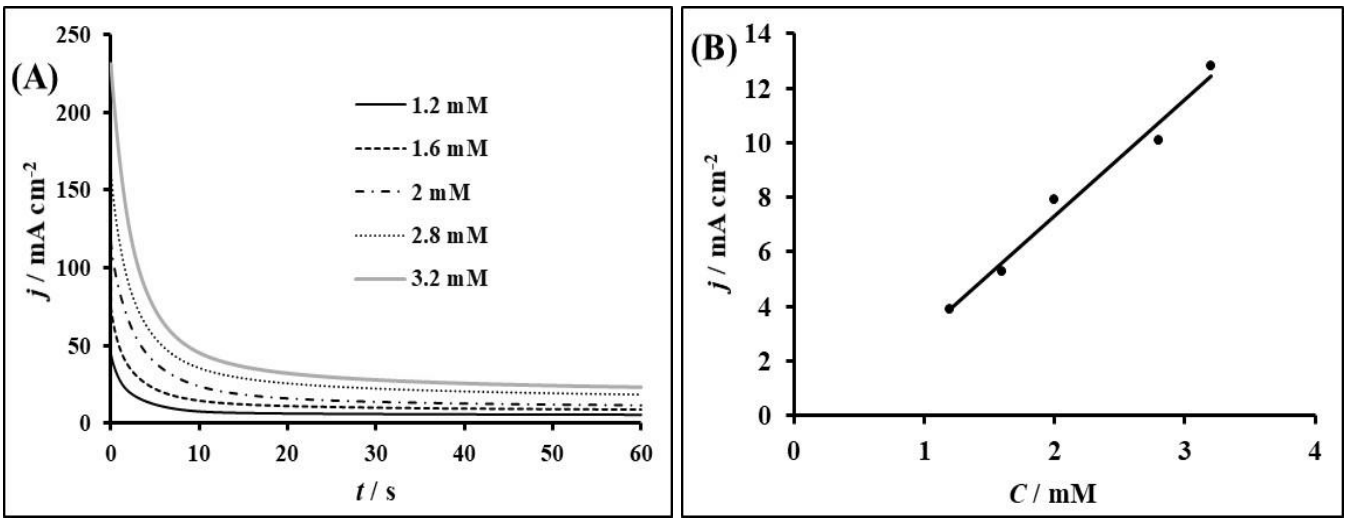

Fig. 9. (A) Chronoamperograms of Ti/RuO_2 in 0.1 M H_2SO_4 (pH = 9) in the presence of several OMP concentrations. Applied potential E = 1 V vs. SCE; (B) Current density versus OMP concentration curve.

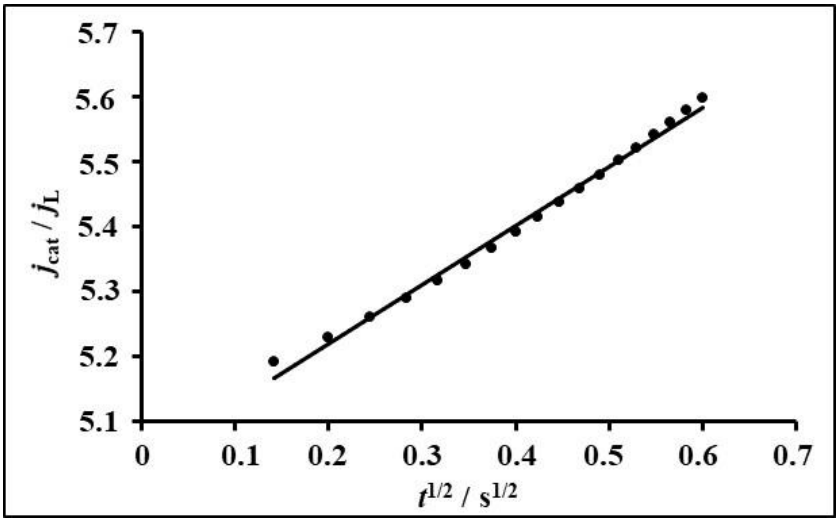

Fig. 10. Curve j_{cat} / j_L vs. $t^{1/2}/s^{1/2}$.

4. Conclusion

The physical characterization of the Ti/RuO_2 electrode showed that it has a rough and cracked structure with the presence of pores on its surface. The electrochemical study showed that the OMP oxidation is done following a direct electronic transfer on the surface of the Ti/RuO_2 electrode. It was also shown that the catalytic oxidation of OMP is controlled by an adsorption-diffusion coupling of the electroactive species on the electrode surface. The influence of temperature revealed the activation of several active sites on the electrode surface as well as the intervention of hydroxyl radicals in the catalytic electrooxidation process of OMP with increasing temperature. The study of the pH influence showed that the process of OMP electrooxidation includes the exchange of three protons and five electrons in acidic media and two protons and one electron exchanged in basic media. The values of activation energy, catalytic rate constant were estimated as 7.895 kJ/mol and 82.2 M^{-1} s^{-1}, respectively.

Aknowledgements

We are thankful to the Swiss National Funds for its financial support. They funded the project (IZ01Z0_146919) which durability helped this work to be undertaken.

References

[1] K.E. Kouadio, O. Kambiré, K.S. Koffi, L. Ouattara, *Electrochemical oxidation of paracetamol on boron-doped diamond electrode: analytical performance and paracetamol degradation*, J. Electrochem. Sci. Eng. 11(2) (2021) 71-86.
DOI: https://doi.org/10.5599/jese.932.

[2] O. Kambiré, L.A.G. Pohan, S.P. Sadia, K.E. Kouadio, L. Ouattara, *Voltammetric study of formic acid oxidation via active chlorine on IrO_2/Ti and RuO_2/Ti electrodes*, Mediterranean Journal of Chemistry 10(8) (2020) 799-808.

[3] G.C. Quand-Meme, A.F.T. Auguste, L.E.M. Hélène, B. Mohamed, S.S. Placide, I. Sanogo, L. Ouattara, *Electrooxidation of ceftriaxone in its commercial formulation on boron doped diamond anode*. J. Adv. Electrochem. 2(2) (2016) 85–88.
https://doi.org/10.4236/ajac.2019.1011039Y.

[4] O. Kambiré, K.S.P. Alloko, L.A.G. Pohan, K.S. Koffi, L. Ouattara, *Electrooxidation of the Paracetamol on Boron Doped Diamond Anode Modified by Gold Particles*, International Research Journal of Pure & Applied Chemistry 22(4) (2021) 23-35.
DOI: 10.9734/IRJPAC/2021/v22i430401.

[5] C.Q.-M. Gnamba, F.T.A. Appia, E.M.H. Loba, I. Sanogo, L. Ouattara, *Electrochemical oxidation of amoxicillin in its pharmaceutical formulation at boron doped diamond (BDD) electrode*, J. Electrochem. Sci. Eng. 5(2) (2015) 129-143. doi: 10.5599/jese.186.

[6] C.-Y. Hu, Y.-Z. Hou, Y.-L. Lin, Y.-G. Deng, S.-J. Hua, Y.-F. Du, C.-W. Chen, C.-H. Wu. *Investigation of iohexol degradation kinetics by using heat-activated persulfate*, Chemical Engineering Journal 379(122403) (2020). http://dx.doi.org /10.1016/j.cej.2019.122403.

[7] S.E. Duirk, C. Lindell, C.C. Cornelison, J. Kormos, T. Ternes, A. Thomas, M. Attene-Ramos, *Formation of toxic iodinated disinfection by-products from compounds used in medical imaging*, Environ. Sci. Technol. 45 (2011) 6845–6854. https://doi.org/10.1021/es200983f.

[8] K.S. Koffi, T.A.A. Foffié, K.E. Kouadio, K.J. Kimou, S. Kone, L. Ouattara, *Cyclic and differential pulse voltammetry investigations of an iodine contrast product using microelectrode of BDD*, Mediterranean Journal of Chemistry 11(3) (2021) 244-254. http://dx.doi.org/10.13171/mjc02109301594.

[9] O. Turkay, S. Barisci, E. Ulusoy, A. Dimoglo, *Electrochemical Reduction of X-ray Contrast Iohexol at Mixed Metal Oxide Electrodes: Process Optimization and By-product Identification*, Water Air Soil Pollut. 229 (2018) 170. https://doi.org/10.1007/s11270-018-3823-0.

[10] Z. Wang, Y.-L. Lin, B. Xu, S.-J. Xia, T.-Y. Zhang, N.-Y. Gao, *Degradation of iohexol by UV/chlorine process and formation of iodinated trihalomethanes during post-chlorination*, Chemical Engineering Journal 283 (2016) 1090–1096. https://doi.org/10.1016/j.cej.2015.08.043.

[11] W. Bottinor, P. Polkampally, I. Jovin, Adverse reactions to iodinated contrast media, Int. J. Angiol. 22 (2013) 149–154. https:// doi.org/10.1055/s-0033-1348885.

[12] K.R. Beckett, A.K. Moriarity, J.M. Langer, *Safe use of contrast media: what the radiologist needs to know*, Radiographics 35 (2015) 1738–1750. https://doi.org/10.1148/rg. 2015150033.

[13] S. Giannakis, M. Jovic, N. Gasilova, M.P. Gelabert, S. Schindelholz, J.-M. Furbringer, H. Girault, C. Pulgarin, *Iohexol degradation in wastewater and urine by UV-based Advanced Oxidation Processes (AOPs): Process modeling and by-products identification*, Journal of Environmental Management, 195(2) (2017) 174-185. https://doi.org/10.1016/j.jenvman.2016.07.004.

[14] S. Papoutsakis, Z. Afshari, S. Malato, C. Pulgarin, *Elimination of the iodinated contrast agent iohexol in water, wastewater and urine matrices by application of photo-Fenton and ultrasound advanced oxidation processes*, Journal of Environmental Chemical Engineering 3(3) (2015) 2002–2009. doi:10.1016/j.jece.2015.07.002.

[15] O. Kambiré, Y.U. Kouakou, A. Kouyaté, S.P. Sadia, K.E. Kouadio, K.J. Kimou, S. Koné, *Removal of rhodamine B from aqueous solution by adsorption on corn cobs activated carbon*, Mediterranean Journal of Chemistry 11(3) (2021) 271-281.

[16] B. Coulibaly, L.A.G. Pohan, O. Kambiré, L.P.S. Kouakou, H. Goure-Doubi, D. Diabaté, L. Ouattara, *Valorization of Green Clay from Bouaflé (Ivory Coast) in the Simultaneous Elimination of Organic Pollutants and Metallic Trace Elements by Adsorption: Case of Methylene Blue and Cadmium Ions*, Chemical Science International Journal 29(8) (2020) 37-51. DOI: 10.9734/CSJI/2020/v29i830199.

[17] Y.U. Kouakou, O. Kambiré, U.P. Gnonsoro, N.S. Eroi, A. Trokourey, *Degradation of Remazol Black dye from Aqueous Solution by Heterogeneous $NH_3(MoO_3)_3/H_2O_2$ System*, International Research Journal of Pure & Applied Chemistry 22(7) 2021) 67-78. DOI: 10.9734/IRJPAC/2021/v22i730421.

[18] P. Yan, Z. Chen, S. Wang, Y. Zhou, J. Shen, S. Zhao, L. Yuan, W. Wang, X. Xu, X. Zhu, J. Kang, *Formation of toxic iodinated by-products during the oxidation process of iohexol by catalytic ozonation in water*, Separation and Purification Technology 262 (118287) (2021). https://doi.org/10.1016/j.seppur.2020.118287.

[19] A.L.G. Pohan, L. Ouattara, K.H. Kondro, O. Kambiré, A. Trokourey, *Electrochemical Treatment of the Wastewaters of Abidjan on Thermally Prepared Platinum Modified Metal Oxides Electrodes*, European Journal of Scientific Research 94 (1) (2013),96-108.

[20] F.T.A. Appia, M. Berté, L. Ouattara, Electrooxidation of amoxicillin on a $Ti/Ta_2O_5/Pt\text{-}RuO_2\text{-}IrO_2$ electrode, RAMReS Sciences des structures et de la Matière 2 (2020) 35-49.

[21] M. Berté, F.T.A. Appia, I. Sanogo, L. Ouattara, *Electrochemical Oxidation of the Paracetamol in its Commercial Formulation on Platinum and Ruthenium Dioxide Electrodes*, Int. J. Electrochem. Sci. 11 (2016), 7736–7749. http://dx. doi: 10.20964/2016.09.44.

[22] O. Kambiré, L.A.G. Pohan, Y.U. Kouakou, K.J. Kimou, K.S. Koffi, K.E. Kouadio, L. Ouattara, *Influence of the coupling of IrO_2 and PtOx on the charging / discharging process at the electrode / electrolytic solution interface*, International Journal of Innovation and Applied Studies 31(3) (2020) 655-667.

[23] F.T.A. Appia, C.Q.-M. Gnamba, O. Kambiré, M. Berté, S.P. Sadia, I. Sanogo, L. Ouattara, *Electrochemical Oxidation of Amoxicillin in Its Commercial Formulation on Thermally Prepared RuO_2/Ti*, J. Electrochem. Sci. Technol. 7(1) (2016) 82-89.

[24] O. Kambire, F.T.A. Appia, L. Ouattara, *Oxygen and chlorine evolution on ruthenium dioxide modified by platinum in acid solutions*, Rev. Ivoir. Sci. Technol. 25 (2015) 21-33.

[25] A. Murthy, A. Manthiram, *Electrocatalytic oxidation of methanol to soluble products on polycrystalline platinum: Application of convolution potential sweep voltammetry in the estimation of kinetic parameters*, Electrochimica Acta 56 (17) (2011) 6078-6083. https://doi.org/10.1016/j.electacta.2011.04.078.

[26] E. Wudarska, E. Chrzescijanska, E. Kusmierek, J. Rynkowski, *Voltammetric studies of acetylsalicylic acid electrooxidation at platinum electrode*, Electrochimica Acta 93 (2013) 189–194. http://dx.DOI: 10.1016/j.electacta.2013.01.107.

[27] P.S. Nagaraj, J.M. Shweta, T.N. Sharanappa, *Electrochemical behavior of an antiviral drug acyclovir at fullerene-C60-modified glassy carbon electrode*, Bioelectrochemistry 88 (2012) 76-83. https://doi.org/10.1016/j.bioelechem.2012.06.004.

[28] A. Masek, E. Chrzescijanska, M. Zaborski, *Electrooxidation of morin hydrate at a Pt electrode studied by cyclic voltammetry*, Food Chemistry 148 (2014) 18–23. https://doi.org/10.1016/j.foodchem.2013.10.003.

[29] A. Masek, E. Chrzescijanska, M. Zaborski, *Estimation of the Antioxidative Properties of Amino Acids – an Electrochemical Approach*, Int. J. Electrochem. Sci. 9 (2014) 7904–7915.

[30] D. Wang, J. Liu, Z. Wu, J. Zhang, Y. Su, Z. Liu, C. Xu, Electrooxidation of Methanol, Ethanol and 1-Propanol on Pd Electrode in Alkaline Medium, Int. J. Electrochem. Sci. 4 (2009) 1672–1678.

[31] N. Belhadj–Tahar, A. Savall, *Mechanistic Aspect of Phenol Electrochemical Degradation by oxidation on a Ta/PbO_2 Anode*, J. electrochem. Soc. 145 (1998) 3427-3434. https://doi.org/10.1149/1.1838822.

[32] Y. Samet, S.C. Elaoud, S. Ammar, R. Abdelhedi, *Electrochemical degradation of 4-chloroguaiacol for waste water treatment using PbO_2 anodes*, Journal of Hazardous Materials 138 (2006) 614-619. https://doi.org/10.1016/j.jhazmat.2006.05.100.

[33] R. Jiménez-Pérez, J. M. Sevilla, T. Pineda, M. Blázquez, J. Gonzalez-Rodriguez, *Study of the electro-oxidation of a recreational drug GHB (gamma hydroxybutyric acid) on a platinum catalyst-type electrode through chronoamperometry and spectro-electrochemistry*, Journal of Electroanalytical Chemistry 766 (2016) 141-146. https://doi.org/10.1016/j.jelechem.2016.02.005.

[34] J. Kimou, O. Kambiré, K.S. Konan, K.E. Kouadio, S. Koné, L. Ouattara, *Electrooxidation of Iohexol in Its Commercial Formulation Omnipaque on Boron Doped Diamond Electrode*, Int. Res. J. Pure Appl. Chemistry 22(11) (2021) 29-41.

[35] J.L.N Xavier, E. Ortega, J.Z. Ferreira, A.M. Bernardes, V. Pérez-Herranz, *An electrochemical Study of Phenol Oxidation in Acidic Medium*, Int. J. Electrochem. Sci. 6 (2011) 622–636.

[36] A. Farahi, H. Hammani, A. Kajai, S. Lahrich, M. Bakasse, M.A. El Mhammedi, *Electro-catalytic detection of dopamine at carbon paste electrode modified with activated carbon: analytical application in blood samples*, International Journal of Environmental Analytical Chemistry (2019).
DOI: 10.1080/03067319.2019.1636043.

[37] R. Zhang, L. Liu, Y. Li, W. Wang, R. Li. *Electrooxidation Kinetics of Hydrazine on Y-type Zeolite-encapsulated Ni(II) (salen) Complex Supported on Graphite Modified Electrode*, Int. J. Electrochem. Sci., 10 (2015) 2355–2369.